
Biological representation disentanglement of single-cell data

SUPPLEMENTARY INFORMATION

Zoe Piran¹, Niv Cohen¹, Yedid Hoshen¹, and Mor Nitzan^{1,2,3,*}

¹School of Computer Science and Engineering, The Hebrew University of Jerusalem, Israel

²Racah Institute of Physics, The Hebrew University of Jerusalem, Israel

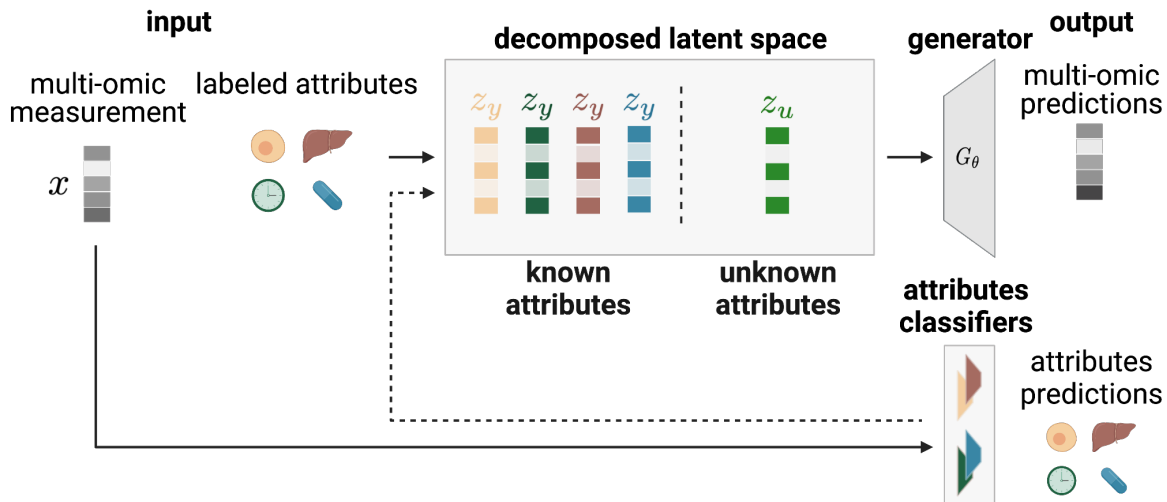
³Faculty of Medicine, The Hebrew University of Jerusalem, Israel

*mor.nitzan@mail.huji.ac.il

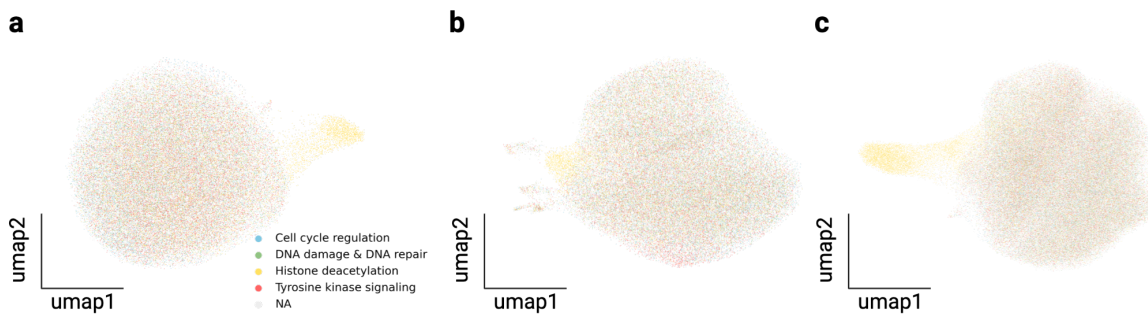
Contents

Supplementary Figures	2
Supplementary Note 1	6
sci-Plex 3	6
Supplementary Note 2	10
Spatio-temporal single-cell atlas of the Plasmodium liver stage	10

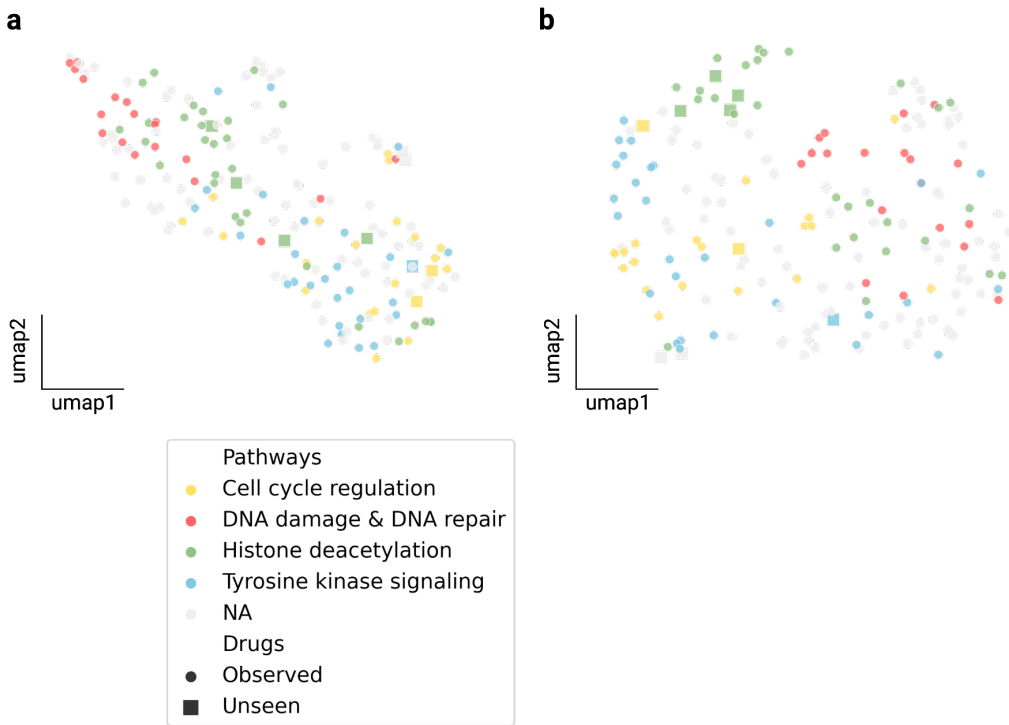
Supplementary Figures



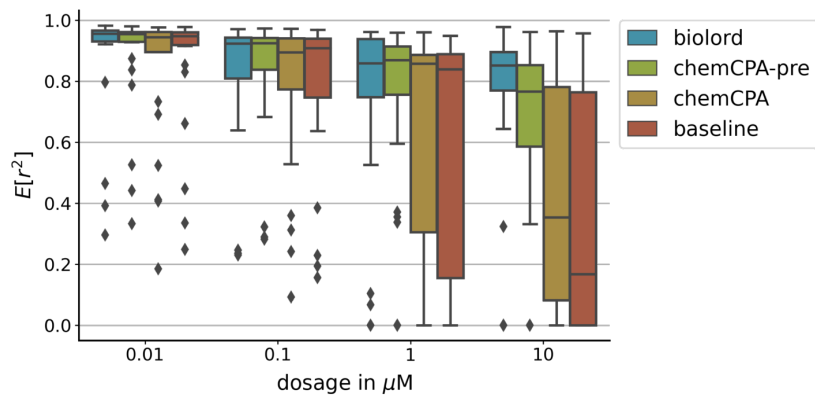
Supplementary Figure 1: A schematic illustration of biolord-classify. The semi-supervised biolord architecture. To handle partial labels we add classifiers to the naive biolord model (see Methods).



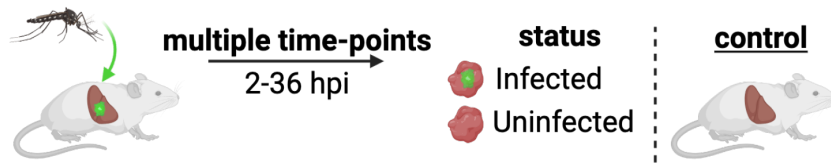
Supplementary Figure 2: The sci-Plex 3 dataset¹. (a)-(c) UMAPs of the original data separated by cell-lines according (a) A549 (lung adenocarcinoma), (b) K562 (chronic myelogenous leukemia), and (c) MCF7 (mammary adenocarcinoma). Cells are colored by pathway associated with the drug-treated.



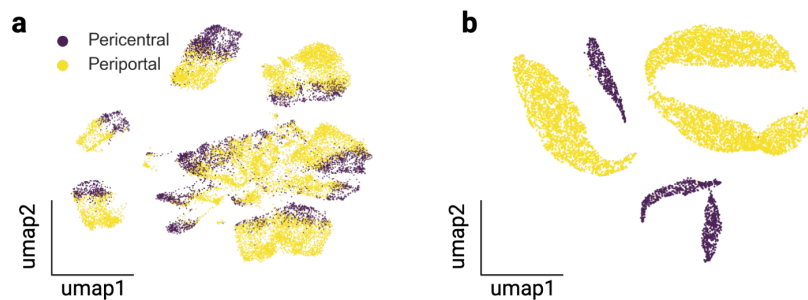
Supplementary Figure 3: biolord decomposed latent space of the sci-Plex 3 dataset¹ exposes drug features. (a) A UMAP of the chemically informed RDKit features used as input for biolord. (b) A UMAP of biolord's drug embedding on the highest dosage ($10 \mu M$). In both UMAPS, Dots, representing drugs, are colored according to known pathways. The shape represents whether the drug is *observed* (circle) or *unseen* (square).



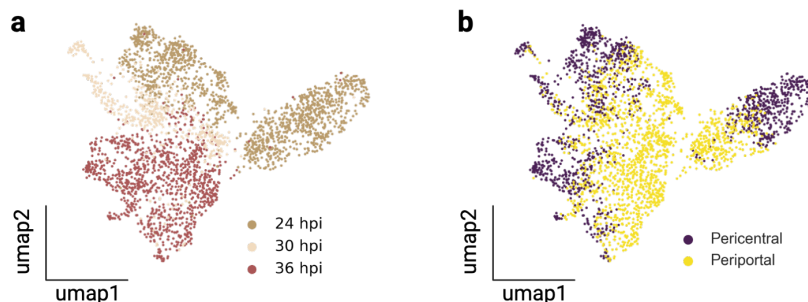
Supplementary Figure 4: Benchmarking performance over the sci-Plex 3 dataset¹. The mean R^2 score, over the nine unseen drugs and all genes. The score is reported for biolord, chemCPA pre-trained model (chemCPA-pre), the standard chemCPA (chemCPA), and the naive baseline (see Methods).



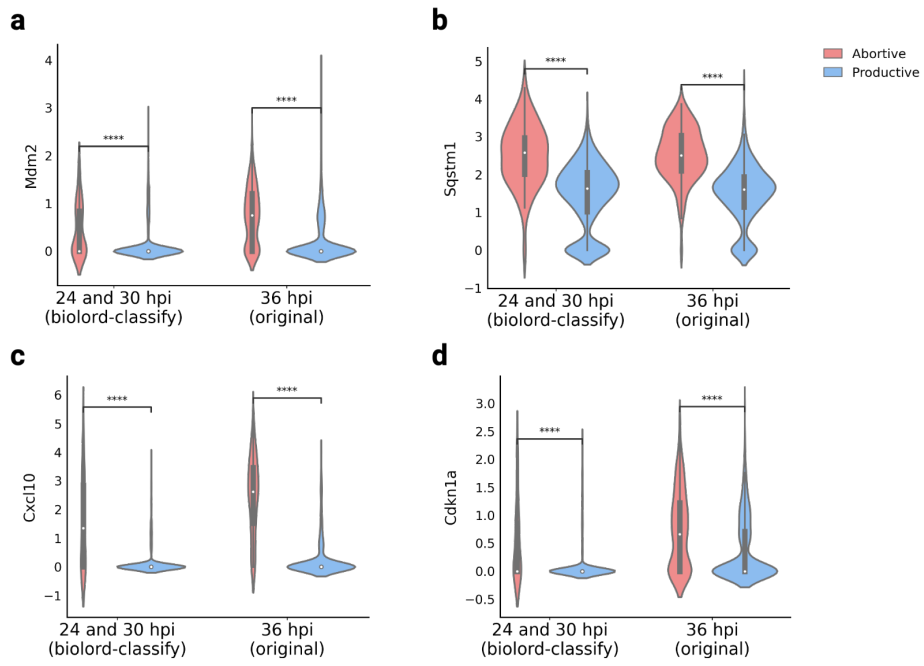
Supplementary Figure 5: The single-cell atlas of the Plasmodium liver stage². Experimental schematic. GFP+ parasites are injected into mice and liver samples are extracted at different time points. Hepatocytes are classified as infected/uninfected using FACS sorting. Control samples are collected from healthy mice.



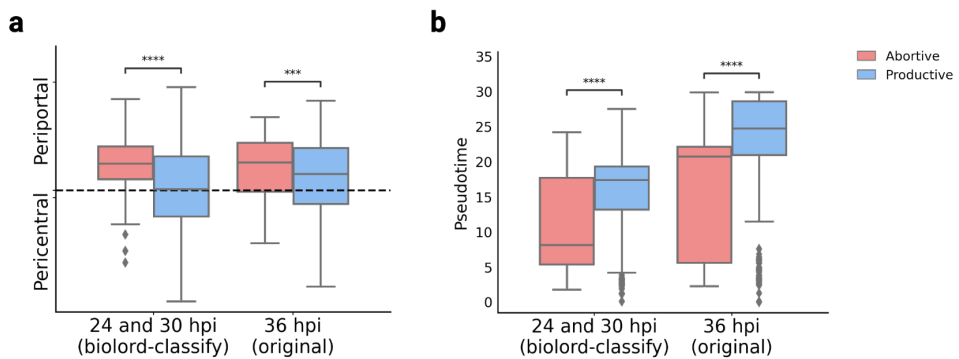
Supplementary Figure 6: Zonation signature in counterfactual predictions of Plasmodium infection². (a) UMAP of the single-cell atlas of the Plasmodium liver stage; cells are colored by spatial zone. (b) UMAP of the original control cells with their counterfactual predictions (c-pred.) for infected/uninfected state; cells are colored by spatial zone.



Supplementary Figure 7: Application of biolord-classify to late time points in the Plasmodium liver stage atlas². (a)-(b) UMAP of cells from late time points; cells colored by (a) hours post-infection or (b) spatial zone.



Supplementary Figure 8: Gene expression patterns are recovered in abortive hepatocytes identified by biolord-classify. Violin plots of representative genes upregulated in abortive hepatocytes. Mann-Whitney-Wilcoxon test two-sided with Benjamini-Hochberg correction P-values: (a) *Mdm2*; 24 and 30 hpi (biolord-classify): 2.786e-12, 36 hpi (original): 8.544e-47, (b) *Sqstm1*; 24 and 30 hpi (biolord-classify): 1.035e-14, 36 hpi (original): 1.27e-63, (c) *Cxcl10*; 24 and 30 hpi (biolord-classify): 7.201e-36, 36 hpi (original): 1.557e-117,(d) *Cdkn1a*; 24 and 30 hpi (biolord-classify): 3.71e-28, 36 hpi (original): 3.04e-17.



Supplementary Figure 9: Global features are preserved in abortive hepatocytes identified by biolord-classify. Boxplots comparing abortive and productive cells show that (a) abortive hepatocytes are more periportally zoned compared with productive hepatocytes; the y axis represents zonation score and scores corresponding to Periportal/Pericentral spatial zones are indicated (see Methods, Mann-Whitney-Wilcoxon test two-sided with Benjamini-Hochberg correction P-values: 24 and 30 hpi (biolord-classify): 6.546e-05, 36 hpi (original): 3.056e-04). (b) The abortive population is concentrated at early pseudotime. Pseudotime was evaluated over parasite mRNA (Afriat et al. 2022) (Mann-Whitney-Wilcoxon test two-sided with Benjamini-Hochberg correction P-values: 24 and 30 hpi (biolord-classify): 1.165e-07, 36 hpi (original): 2.715e-35).

Supplementary Note 1

sci-Plex 3

biolord. For all biolord models of the sci-Plex 3 dataset¹ we use the same anndata file available on figshare ([sciplex3](#)) and the biolord model settings as listed in Table 1. We used Weights & Biases³ for experiment tracking and hyper-parameter tuning. To cover the large space of possible configuration space we tuned subsets of the parameters in consecutive iterations (Table 2). We started with tuning the more dominant parameters. For example, "loss_ae" or architecture parameters such as "n_latent", and "{}_depth" or "{}_width" parameters. We next tuned the loss parameters (e.g., penalties strength) and the dropout rate. Finally, we tuned the finer optimization parameters such as the learning rates and regularization parameters. We randomized over valid values for the inspected parameters at each iteration and kept the ones that consistently outperformed. The range of values scanned for each parameter and the best configurations are given in Table 2.

Table 1: General settings for a biolord model on the sci-Plex 3 data¹.

Parameter	Value
ordered_attributes_keys	["rdkit2d_dose"]
discrete_attributes_keys	["cell_type"]
train_classifiers	False
batch_size	512
split_key	"split_ood"
max_epochs	500
early_stopping	True
loss_ae	"gauss"

chemCPA. For the non-pre-trained version, we follow the parameters supplied in '[finetuning_num_genes.json](#)' ('_id = 1007')⁴. The parameters are presented in Table 3.

ChemCPA-pre. For the pre-trained version, we followed '[finetuning_num_genes.json](#)'⁴ ('_id = 789'). As advised by the authors we tune the adversarial parameters, as detailed in Table 4.

Table 2: Parameters range for the biolord sweep on the sci-Plex 3 data¹ and optimal configuration used.

Parameter	Values	Best config
n_latent	[16,32,64,128]	256
n_latent_attribute_ordered	[128,256,512]	256
n_latent_attribute_discrete	[2,3,4,6,8]	3
autoencoder_width	[32,64,128,256,512,1024,2048,4096]	4096
autoencoder_depth	[1,2,3,4,6,8]	4
autoencoder_lr	[1×10^{-2} , 1×10^{-3} , 1×10^{-4}]	1×10^{-4}
autoencoder_wd	[1×10^{-2} , 1×10^{-3} , 1×10^{-4}]	1×10^{-4}
attribute_nn_width	[32,64,128,256,512,1024,2048,4096]	2048
attribute_nn_depth	[1,2,3,4,6,8]	2
attribute_nn_lr	[1×10^{-2} , 1×10^{-3} , 1×10^{-4}]	1×10^{-2}
attribute_nn_wd	[1×10^{-8} , 4×10^{-8} , 1×10^{-7}]	4×10^{-8}
unknown_attribute_noise_param	[0.1, 0.5, 1, 2, 5, 10, 20]	20
reconstruction_penalty	[1×10^{-2} , 1×10^{-1} , 1×10^0 , $1, 1 \times 10^2$, 5×10^3 , 1×10^4]	1×10^4
unknown_attribute_penalty	[0.1, 1, 2, 5, 10, 20, 50, 100, 200]	0.1
step_size_lr	[45, 90, 180]	45
use_batch_norm	[True, False]	False
use_layer_norm	[True, False]	False
cosine_scheduler	[True, False]	True
attribute_dropout_rate	[0.05,0.1,0.25,0.5,0.75]	0.1
scheduler_final_lr	[1×10^{-3} , 1×10^{-4} , 1×10^{-5} , 1×10^{-6} ,]	1×10^{-5}

Table 3: Hyperparameters used for reported chemCPA results on the sci-Plex 3 data¹.

Parameter	Value
num_epochs	200
patience	50
dim	32
dropout	2.624×10^{-1}
autoencoder_width	256
autoencoder_depth	4
autoencoder_lr	1.575×10^{-3}
autoencoder_wd	6.251×10^{-7}
adversary_width	128
adversary_depth	3
adversary_lr	8.060×10^{-4}
adversary_wd	4.000×10^{-6}
reg_adversary	9.101×10^0
reg_adversary_cov	1.068×10^1
penalty_adversary	4.550×10^{-1}
batch_size	32
dosers_width	64
dosers_depth	3
dosers_lr	1.575×10^{-3}
dosers_wd	6.251×10^{-7}
embedding_encoder_width	128
embedding_encoder_depth	4
append_ae_layer	True
enable_cpa_mode	False
reg_multi_task	0

Table 4: Parameters range for the chemCPA-pre sweep on the sci-Plex 3 data¹ and optimal configuration used.

Parameter	Values	Best config
num_epochs	-	200
patience	-	50
dim	-	32
dropout	-	2.624×10^{-1}
autoencoder_width	-	256
autoencoder_depth	-	4
autoencoder_lr	-	2.051×10^{-4}
autoencoder_wd	-	2.940×10^{-8}
reg_adversary_cov	-	4.176
batch_size	-	32
dosers_width	-	64
dosers_depth	-	3
dosers_lr	-	2.051×10^{-4}
dosers_wd	-	2.940×10^{-8}
embedding_encoder_width	-	128
embedding_encoder_depth	-	4
append_ae_layer	-	True
enable_cpa_mode	-	False
reg_multi_task	-	0
adversary_width	[64, 128, 256]	256
adversary_depth	[2, 3, 4]	3
adversary_lr	$(5 \times 10^{-5}, 1 \times 10^{-2})$	1.143×10^{-4}
adversary_wd	$(1 \times 10^{-8}, 1 \times 10^{-2})$	4×10^{-6}
adversary_steps	[2, 3]	2
reg_adversary	(5, 100)	1.778
penalty_adversary	(0.5, 5)	8.89×10^{-2}

Supplementary Note 2

Spatio-temporal single-cell atlas of the Plasmodium liver stage

As described in the main text we define two biolord settings for the analysis of the spatio-temporal single-cell atlas of the Plasmodium liver stage². Below we provide the model details for each case.

Infected state analysis using counterfactual predictions

The relevant anndata file can be downloaded from figshare ([spatio-temporal-infection_infected](#)). The setting for the biolord model is provided in Table 5 and hyperparameter choice in Table 6. Of note, parameters relating to ordered attributes are missing as we do not have ordered attributes.

Table 5: The setting for the biolord model for the infected state analysis.

Parameter	Value
discrete_attributes_keys	["time_int", "status_control", "zone"]
train_classifiers	False
batch_size	512
split_key	"split_random"
max_epochs	500
early_stopping	True
early_stopping_patience	20

Table 6: Parameters of the biolord model used for the infected state analysis.

Parameter	Value
n_latent	32
n_latent_attribute_discrete	4
autoencoder_width	1024
autoencoder_depth	4
autoencoder_lr	1×10^{-4}
autoencoder_wd	1×10^{-4}
unknown_attribute_noise_param	1×10^{-1}
reconstruction_penalty	1×10^2
unknown_attribute_penalty	1×10^1
step_size_lr	45
use_batch_norm	False
use_layer_norm	False
cosine_scheduler	True
attribute_dropout_rate	0.1
scheduler_final_lr	1×10^{-5}
loss_ae	"gauss"

Abortive state classification

The relevant anndata file can be downloaded from figshare ([spatio-temporal-infection_abortive](#)), named 'spatio-temporal-infection_abortive'. The setting for the biolord model is provided in Table 7 and hyperparameter choice in Table 8.

Table 7: The setting for the biolord model for the abortive state analysis.

Parameter	Value
ordered_attributes_keys	["stress_score"]
discrete_attributes_keys	["time_int", "abortive_state", "zone"]
categorical_attributes_missing	{"time_int": None, "abortive_state": "Unknown", "zone": None}
train_classifiers	True
batch_size	256
split_key	"split_random"
max_epochs	500
early_stopping	True
early_stopping_patience	20

Table 8: Parameters of the biolord model used for the infected state analysis.

Parameter	Value
n_latent	32
n_latent_attribute_discrete	4
n_latent_attribute_ordered	16
autoencoder_width	512
autoencoder_depth	4
autoencoder_lr	1×10^{-4}
autoencoder_wd	1×10^{-4}
attribute_nn_width	512
attribute_nn_depth	4
attribute_nn_lr	1×10^{-2}
attribute_nn_wd	4×10^{-8}
unknown_attribute_noise_param	1×10^{-1}
reconstruction_penalty	1×10^2
unknown_attribute_penalty	1×10^1
step_size_lr	90
use_batch_norm	False
use_layer_norm	False
cosine_scheduler	True
attribute_dropout_rate	0.05
scheduler_final_lr	1×10^{-5}
loss_ae	"gauss"
loss_ordered_attribute	"gauss"
classification_penalty	0
classifier_dropout_rate	1×10^{-1}
classifier_penalty	1×10^1
classify_all	False

References

- [1] Sanjay R Srivatsan, et al. Massively multiplex chemical transcriptomics at single-cell resolution. *Science*, 367(6473):45–51, 2020.
- [2] Amichay Afriat, et al. A spatiotemporally resolved single-cell atlas of the plasmodium liver stage. *Nature*, pages 1–7, 2022.
- [3] Lukas Biewald. Experiment tracking with weights and biases, 2020. URL <https://www.wandb.com/>. Software available from wandb.com.
- [4] Leon Hetzel, et al. Predicting cellular responses to novel drug perturbations at a single-cell resolution. In *Advances in Neural Information Processing Systems*, 2022.